

# Astroglial Expression of Human $\alpha_1$ -Antichymotrypsin Enhances Alzheimer-like Pathology in Amyloid Protein Precursor Transgenic Mice

Lennart Mucke,<sup>\*†‡</sup> Gui-Qiu Yu,<sup>\*</sup>  
Lisa McConlogue,<sup>¶</sup> Edward M. Rockenstein,<sup>||</sup>  
Carmela R. Abraham,<sup>§</sup> and Eliezer Masliah<sup>||</sup>

From the Gladstone Institute of Neurological Disease,<sup>\*</sup> Department of Neurology,<sup>†</sup> and Neuroscience Program,<sup>‡</sup> University of California San Francisco, San Francisco, California; Elan Pharmaceuticals,<sup>¶</sup> South San Francisco, California; the Departments of Neurosciences and Pathology,<sup>||</sup> University of California at San Diego, La Jolla, California; and the Departments of Biochemistry and Medicine, Boston University School of Medicine,<sup>§</sup> Boston, Massachusetts

**Proteases and their inhibitors play key roles in physiological and pathological processes. Cerebral amyloid plaques are a pathological hallmark of Alzheimer's disease (AD). They contain amyloid- $\beta$  (A $\beta$ ) peptides in tight association with the serine protease inhibitor  $\alpha_1$ -antichymotrypsin.<sup>1,2</sup> However, it is unknown whether the increased expression of  $\alpha_1$ -antichymotrypsin found in AD brains counteracts or contributes to the disease. We used regulatory sequences of the glial fibrillary acidic protein gene<sup>3</sup> to express human  $\alpha_1$ -antichymotrypsin (hACT) in astrocytes of transgenic mice. These mice were crossed with transgenic mice that produce human amyloid protein precursors (hAPP) and A $\beta$  in neurons.<sup>4,5</sup> No amyloid plaques were found in transgenic mice expressing hACT alone, whereas hAPP transgenic mice and hAPP/hACT doubly transgenic mice developed typical AD-like amyloid plaques in the hippocampus and neocortex around 6 to 8 months of age. Co-expression of hAPP and hACT significantly increased the plaque burden at 7 to 8, 14, and 20 months. Both hAPP and hAPP/hACT mice showed significant decreases in synaptophysin-immunoreactive presynaptic terminals in the dentate gyrus, compared with nontransgenic littermates. Our results demonstrate that hACT acts as an amyloidogenic cofactor *in vivo* and suggest that the role of hACT in AD is pathogenic. (Am J Pathol 2000, 157:2003–2010)**

The major protein component of plaques in Alzheimer's disease (AD) brains is amyloid  $\beta$  (A $\beta$ ), which is derived proteolytically from the amyloid protein precursor.<sup>6–8</sup> The majority of A $\beta$  produced in the normal brain terminates at amino acid 40 (A $\beta_{40}$ ).<sup>9</sup> Mutations linked to autosomal

dominant forms of familial AD (FAD) and formation of plaques in all forms of AD are associated with an abnormal accumulation of A $\beta$  ending at amino acid 42 (A $\beta_{42}$ ), which aggregates more readily than A $\beta_{40}$ .<sup>10,11</sup>

High-level neuronal expression of FAD-mutant forms of human amyloid precursor protein (hAPP)/A $\beta$ , directed by the platelet-derived growth factor (PDGF)  $\beta$  chain promoter, elicits age-related synaptic transmission deficits and AD-like neuropathological alterations in transgenic mice, including typical amyloid plaques.<sup>4,5,12–15</sup> AD-like pathology has also been observed in a variety of other transgenic models in which neuronal expression of FAD-mutant hAPP is directed by different promoters.<sup>16</sup>

Diverse proteins bind to amyloid plaques including apolipoprotein E, extracellular matrix proteins, amyloid P component, complement, and cytokines.<sup>17</sup> Most of these proteins also bind to other forms of amyloid (eg, in primary AL amyloidosis, secondary AA amyloidosis, FAP amyloidosis, or prion-associated spongiform encephalopathies). In contrast, human  $\alpha_1$ -antichymotrypsin (hACT) seems to be associated primarily with A $\beta$  amyloidosis,<sup>18</sup> suggesting a more specific role for hACT in AD pathogenesis. However, this role remains to be determined.

ACT is a serine protease inhibitor (serpin) and an acute phase protein.<sup>19</sup> In AD, hACT mRNA levels are increased in the cortex<sup>1</sup> where hACT is produced primarily by astrocytes.<sup>20,21</sup> *In vitro*, hACT increases,<sup>22,23</sup> decreases,<sup>24,25</sup> or does not alter<sup>17,26</sup> amyloid fibril formation. Similarly controversial results have been reported for the effects of hACT on A $\beta$ -induced neurotoxicity.<sup>27–30</sup> Here we demonstrate that astroglial expression of hACT increases amyloid deposition *in vivo* and that this effect does not augment A $\beta$ -induced synaptotoxicity.

## Materials and Methods

### Generation of Transgenic Mice

An ~1.7-kb fragment containing a full-length hACT cDNA<sup>1</sup> was isolated from pGEM4 by *Eco*RI digest, sub-

Supported by National Institutes of Health Grants AG11385 (to L. M.), AG09905 (to C. A.), AG5131 and AG10869 (to E. M.).

Accepted for publication September 8, 2000.

Address reprint requests to Lennart Mucke, M.D., Gladstone Institute of Neurological Disease, P.O. Box 41900, San Francisco, CA 94141-9100. E-mail: Lmucke@gladstone.ucsf.edu.

cloned in pGEMEX-2 after *NotI* linker ligation, and ligated via *NotI* with a glial fibrillary acidic protein (GFAP) expression construct (C-445) described previously.<sup>31</sup> The resulting GFAP-hACT transgene was freed of vector sequences by *SfiI* digestion, purified, and microinjected into C57Bl/6xSJL F2 one-cell embryos. The PDGF-hAPP transgene<sup>12,13</sup> and the generation of PDGF-hAPP line J9 on the C57Bl/6xDBA/2 background<sup>4</sup> have been described.

Mice were crossed as outlined in the Results section and genomic tail DNA was analyzed with a touchdown polymerase chain reaction protocol essentially as described.<sup>32</sup> hACT primers: forward (5'-CTCGAGCTC-GAGAGTTAGTCCTGAAGGCC-3'), reverse (5'-AGATCTAGATCTCGGAGGTGCTGGAAGCTC-3'). hAPP primers: forward (5'-GGTGAGTTTGAAGTGATGCC-3'), reverse (5'-TCTTCTTCTCCACCTCAGC-3'). Genotypes were confirmed by slot-blot analysis with <sup>32</sup>P-labeled cDNA probes specific for hAPP or hACT coding sequences. All transgenic mice were heterozygous with respect to individual transgenes. Nontransgenic littermates served as controls.

### Preparation of Brain Tissues

For analysis, mice were anesthetized with chloral hydrate and flush-perfused transcardially with 0.9% saline. Brains were removed and divided sagittally. One hemibrain was postfixed in phosphate-buffered 4% paraformaldehyde (pH 7.4) at 4°C for 48 hours for vibratome sectioning at 40  $\mu$ m; the other hemibrain was snap-frozen, either in its entirety or after rapid dissection into subregions, and stored at -70°C for RNA and protein analyses. Postmortem brain tissues from humans without neurological disease were obtained from the tissue bank of the Alzheimer's Disease Research Center at the University of California at San Diego.

### RNase Protection Assays

RNA extraction and mRNA quantitation by solution hybridization RNase protection assay were performed as described,<sup>13</sup> using 10  $\mu$ g of total RNA per sample in combination with the following <sup>32</sup>P-labeled antisense riboprobes (protected nucleotides are indicated with reference to GenBank accession numbers): hAPPSV40 containing nucleotides 2468 to 2657 (X06989) of hAPP fused by *NotI* linker with nucleotides 2532 to 2656 (M24914) of SV40, hACT containing nucleotides 200 to 380 (K01500) of hACT, and actin containing nucleotides 480 to 559 (X03672) of mouse  $\beta$ -actin sequence.

### Primary Astrocyte Cultures

Cultures of primary astrocytes were established from whole brains of neonatal mice as described.<sup>33</sup> Cells were grown to confluence, washed in serum- and methionine-free Dulbecco's modified Eagle's medium, placed in t-80 flasks, and labeled with 4 ml of <sup>35</sup>S-methionine (25  $\mu$ Ci/ml) for 18 hours. Conditioned media were then collected

and spun at 100,000  $\times g$  for 1 hour. Supernatants were first precleared with preimmune serum followed by protein A Sepharose and spun at 3,000 rpm in an Eppendorf centrifuge for 5 minutes. The supernatants were collected and hACT was immunoprecipitated for 18 hours at 4°C with polyclonal goat (Atlantic, Stillwater, MN) or rabbit (MBL, Japan) anti-hACT antibodies (diluted 1:500). Complexes were brought down with protein A Sepharose for 1 hour at 4°C. The pellets were rinsed in STEN buffer, boiled in Laemmli sample buffer, and separated by sodium dodecyl sulfate-polyacrylamide gel electrophoresis. The gels were then fixed, enhanced with Enlightening (New England Nuclear, Boston, MA), and autoradiographed. Similar results were obtained with either of the primary antibodies.

### Quantitations of A $\beta$

Snap-frozen hippocampus was homogenized in guanidine buffer, and human A $\beta$  (A $\beta_{1-x}$  versus A $\beta_{1-42}$ ) was quantitated by enzyme-linked immunosorbent assay as described.<sup>15</sup> Sagittal vibratome sections (40  $\mu$ m) of post-fixed hemibrains were incubated overnight at 4°C with biotinylated mouse monoclonal antibody 3D6 (diluted to 5  $\mu$ g/ml; Elan Pharmaceuticals, South San Francisco, CA), which specifically recognizes A $\beta_{1-5}$ .<sup>15,34</sup> Binding of primary antibody was detected with an Elite kit (Vector Laboratories, Burlingame, CA) using diaminobenzidine and H<sub>2</sub>O<sub>2</sub> for development. Sections were counterstained with 1% hematoxylin and examined with a Vanox light microscope (Olympus, Tokyo, Japan) using a  $\times 2.5$  objective. The percent area of the hippocampus covered by 3D6-immunoreactive deposits (plaque load) was determined morphometrically with a Quantimet 570C (Leica, Deerfield, IL) in four immunolabeled sections per mouse. One section per mouse was immunostained and analyzed in each of four independent experiments and average values were calculated from the pooled data. Additional sections were pretreated with formic acid (99%) for 45 seconds and labeled with rabbit polyclonal antibodies (diluted 1:1,000; a gift from Dr. F. Checler, IPMC du CNRS, Valbonne, France) that specifically recognize the C-terminus of A $\beta_{40}$  or A $\beta_{42}$ .<sup>35</sup> Specific binding of these antibodies was detected essentially as described.<sup>34</sup> For detection of mouse A $\beta$ , sections were incubated with the rabbit polyclonal antibody RAT 1-28 (Elan Pharmaceuticals) and then with biotinylated goat anti-rabbit IgG. Immunoperoxidase activity was revealed with an Elite kit (Vector Laboratories) using diaminobenzidine and H<sub>2</sub>O<sub>2</sub> for development.

### Evaluation of Presynaptic Terminals

To ensure objective assessments and reliability of results, brain sections from mice to be compared in any given experiment were blind-coded and processed in parallel. Codes were broken after the analysis was complete. Vibratome sections were labeled with monoclonal antibodies against synaptophysin (1  $\mu$ g/ml; Boehringer-Mannheim, Indianapolis, IN) or GAP-43 (1:100; Sigma)

as described.<sup>36</sup> Synaptophysin-immunofluorescence-labeled sections were imaged with a laser-scanning confocal microscope (MRC1024; Bio-Rad Laboratories, Hercules, CA) as described.<sup>12,14</sup> Three sections were analyzed per mouse and four confocal images (each covering 7,282  $\mu\text{m}^2$ ) of the molecular layer of the dentate gyrus were obtained per section. One section per mouse was immunostained and analyzed in each of three independent experiments and average values were calculated from the pooled data. Digitized images were transferred to a Macintosh computer and analyzed with NIH Image. For each experiment, we first determined the linear range of the intensity of immunoreactive terminals in nontransgenic control sections. This setting was then used, as described,<sup>37</sup> to collect all images analyzed in the same experiment. The area of the outer molecular layer occupied by synaptophysin-immunoreactive (SYN-IR) presynaptic terminals was quantified and expressed as a percentage of the total image area.<sup>12,36</sup> As reviewed recently,<sup>5,37</sup> this method has been used to assess neurodegenerative alterations in diverse experimental models and in diseased human brains and has been validated by comparisons with quantitative immunoblots, quantitations of synaptic proteins by enzyme-linked immunosorbent assay, and the optical disector approach. GAP-43-immunoperoxidase-labeled sections were analyzed microdensitometrically with the Quantimet 570C as described<sup>36</sup> to determine the level of GAP-43 immunoreactivity in the molecular layer of the dentate gyrus.

### Statistical Analysis

Statistical analyses were performed with the StatView 5.0 program (SAS Institute Inc., Cary, NC). Differences among normally distributed sets of data were evaluated by one-way analysis of variance and Tukey-Kramer post hoc test. Differences in plaque load were assessed by the Mann-Whitney *U* test. Correlation studies were performed by simple regression analysis. The null hypothesis was rejected at the 0.05 level.

## Results

### Expression of hACT in Astrocytes of Transgenic Mice

We used regulatory sequences of the murine GFAP gene to target expression of hACT to astrocytes (Figure 1). Six GFAP-hACT transgenic founders were identified and their offspring analyzed for cerebral transgene expression by RNase protection assay. Mice from the highest expresser line (528-13) had robust hACT mRNA levels in the brain (Figure 1b), and primary astrocytes from these mice released hACT into the extracellular milieu (Figure 1c). hACT mice displayed no overt behavioral phenotype, and inspection of their hematoxylin and eosin-stained brain sections revealed a normal cytoarchitecture (data not shown). Line 528-13 was selected for further analysis in this study.

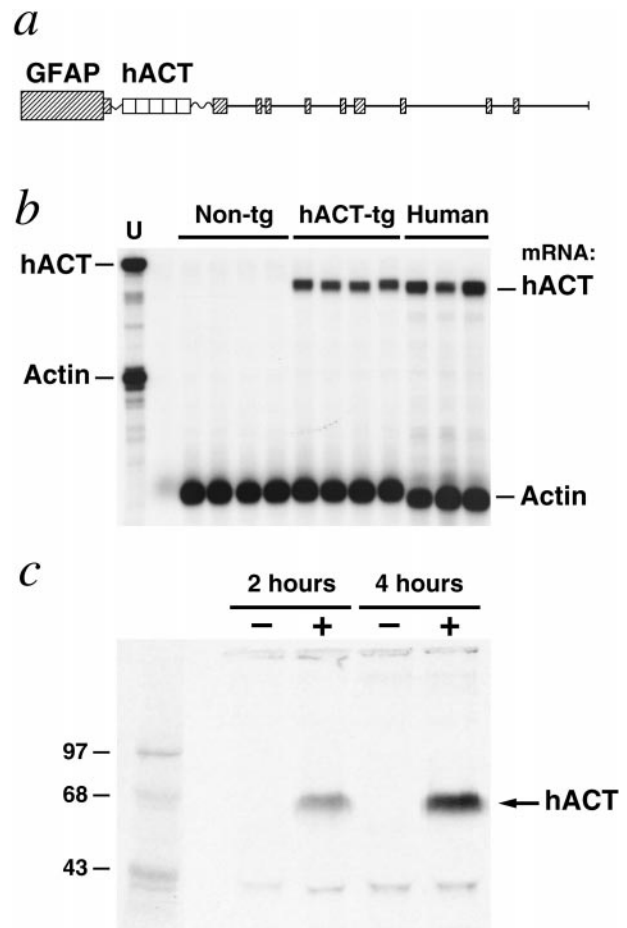


**Figure 1.** Expression of hACT in astrocytes of transgenic mice. **a:** Astroglial expression of an hACT cDNA<sup>1</sup> was directed by regulatory sequences of a modified murine GFAP gene.<sup>3</sup> SV40 polyadenylation signals at the 3' end of the hACT cDNA prevent expression of downstream GFAP-coding sequences. Elements are not drawn to scale. **b:** hACT mRNA levels in brains of humans and transgenic mice. A representative autoradiograph is shown. Total RNA extracted from mouse hemibrains or from the midfrontal gyrus of humans without neurological disease was analyzed by RNase protection assay. The **leftmost lane** shows signals of undigested radiolabeled riboprobes. The other lanes contained the same riboprobes plus brain RNA (10  $\mu\text{g}/\text{lane}$ ) from different mice or humans, digested with RNases. Protected mRNA segments are indicated on the **right**. Non-tg = nontransgenic. Signals were quantitated by phosphorimager analysis: hACT/actin mRNA ratios in hACT mice (0.18, 0.15, 0.17, 0.18) were less variable than those in postmortem human brain tissues (0.18, 0.39, 0.48). **c:** Production of hACT by transgenic astrocytes. Primary astrocytes were established from transgenic (+) and nontransgenic (-) neonatal mice and metabolically labeled for 2 or 4 hours. hACT was immunoprecipitated with anti-hACT antibodies from conditioned culture medium, separated by sodium dodecyl sulfate-polyacrylamide gel electrophoresis, and detected by autoradiography. Results similar to those shown were obtained with a different hACT antibody. The **left lane** contains <sup>14</sup>C-labeled molecular weight standards.

### Astroglial Expression of hACT Increases Amyloid Deposition in hAPP Transgenic Mice

Heterozygous GFAP-hACT transgenic mice (line 528-13) were crossed with heterozygous PDGF-hAPP transgenic mice (line J9<sup>4,5</sup>) expressing an FAD-mutant hAPP mini-gene (Figure 2a) in neurons. These crosses yielded four groups of littermates ( $n = 20$  to 21 per genotype): hACT mice, hAPP mice, hAPP/hACT mice, and nontransgenic controls.



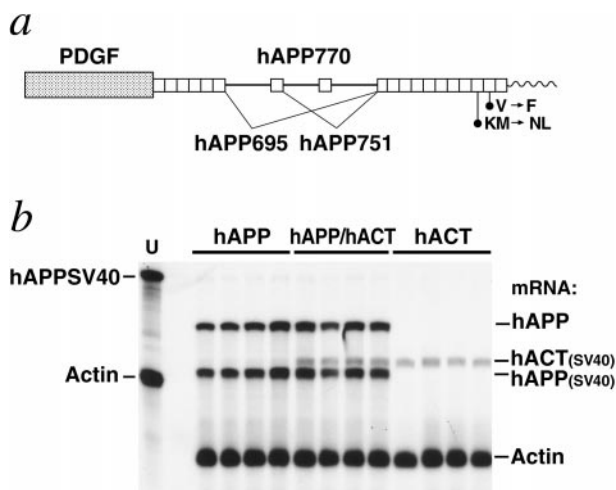


**Figure 2.** Cerebral transgene expression in hAPP/hACT mice and singly transgenic controls. **a:** Neuronal expression of an alternatively spliced hAPP minigene was directed by the human PDGF  $\beta$ -chain promoter as described previously.<sup>12,13</sup> The hAPP minigene expressed in line J9 carries FAD-linked mutations (670/671<sub>KM</sub>  $\rightarrow$  <sub>NL</sub> and 717<sub>V</sub>  $\rightarrow$  <sub>F</sub>, hAPP770 numbering) that increase the production of A $\beta$ <sub>42</sub>.<sup>4,5,10</sup> Elements are not drawn to scale. **b:** hACT expression does not alter cerebral hAPP mRNA levels. A representative autoradiograph is shown. Total RNA extracted from mouse hemibrains was analyzed by RNase protection assay. Conventions are as in Figure 1b. The chimeric hAPPSV40 probe protects human but not mouse amyloid precursor protein; it also protects SV40 sequences in transgene-derived mRNAs. These SV40 sequences provide polyadenylation signals and are of slightly different length in the two transgenes allowing for differentiation of GFAP-hACT-derived (hACT<sub>(SV40)</sub>) and PDGF-hAPP-derived (hAPP<sub>(SV40)</sub>) mRNA segments. Signals were quantitated by phosphorimager analysis: singly and doubly transgenic mice ( $n = 4$  per genotype) did not differ significantly in hAPP/actin ( $0.298 \pm 0.053$  versus  $0.307 \pm 0.096$ ) or hACT<sub>(SV40)</sub>/actin ( $0.153 \pm 0.021$  versus  $0.160 \pm 0.012$ ) mRNA ratios (mean  $\pm$  SD).

Hippocampal deposition of A $\beta$  was assessed in all four groups of mice at 7 to 8, 14, and 20 months of age. No amyloid deposits were detected in hACT mice or non-transgenic controls using antibodies that recognize human or mouse A $\beta$  (data not shown). In contrast, hAPP and hAPP/hACT mice developed AD-like amyloid plaques around 7 months of age, and progressive accumulation of plaques was observed at 14 and 20 months (Figures 3 and 4).

The percent area of the hippocampus covered by A $\beta$ -immunoreactive deposits (plaque load) was determined morphometrically as described in Materials and Methods. At all ages analyzed, hAPP/hACT mice had a higher plaque load than hAPP mice (Figure 4). The distribution of the plaques was similar in both groups (Figure 3 and data not shown). Diffuse amyloid deposits first developed in a laminar distribution in the molecular layer of the dentate gyrus and the hippocampal alveus, followed by the formation of more mature compact plaques (3 to 15  $\mu$ m in diameter) in the stratum radiatum of the hippocampus, the subiculum, and the neocortex. Areas that are relatively spared in AD, such as the thalamus, basal ganglia, and cerebellum, displayed only occasional small amyloid deposits ( $\leq 5$   $\mu$ m in diameter) in these mice. Plaques in both hAPP and hAPP/hACT mice showed stronger immunoreactivity for A $\beta$ <sub>42</sub> than for A $\beta$ <sub>40</sub> (data not shown), consistent with results obtained in humans.<sup>11</sup> In contrast to hACT mice and nontransgenic controls, hAPP and hAPP/hACT mice developed a reac-

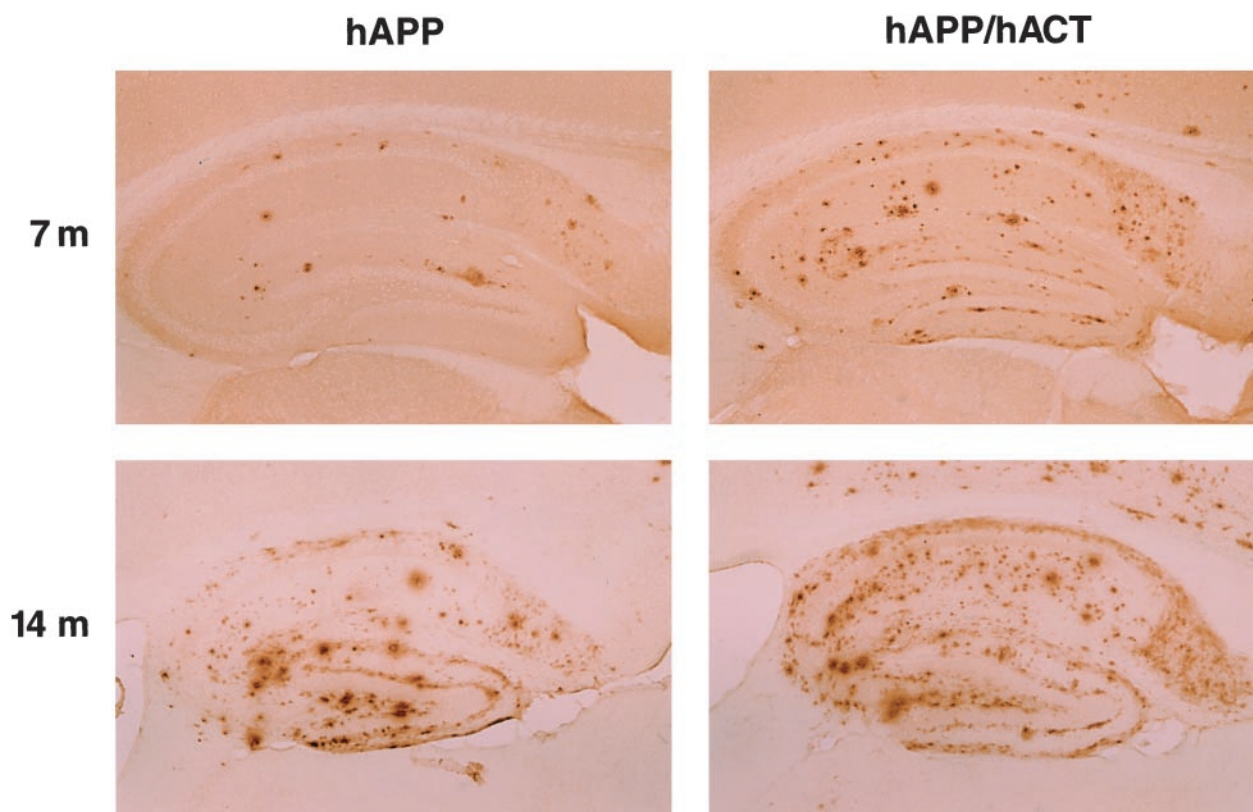


**Figure 3.** Astroglial expression of hACT increases amyloid deposition in hAPP/hACT mice. Brain sections from hAPP mice (**left**) and hAPP/hACT mice (**right**) were labeled with the anti-A $\beta$  antibody 3D6 at 7 or 14 months (m) of age. A $\beta$ -immunoreactive deposits in the hippocampus were visualized by immunoperoxidase reaction and light microscopy.

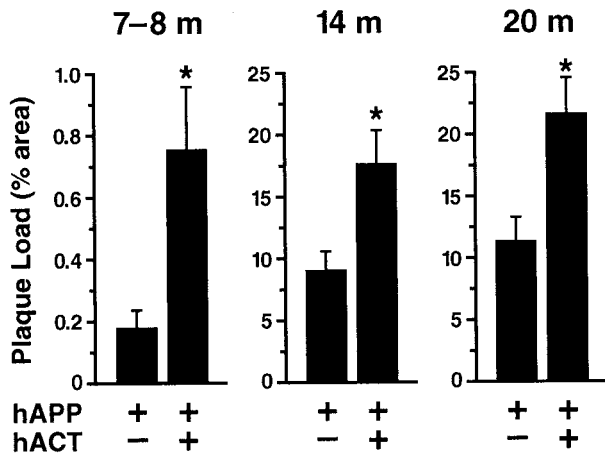


**Figure 4.** Quantitation of plaque load in hAPP and hAPP/hACT mice at different ages. Brain sections of hAPP and hAPP/hACT mice were labeled with the 3D6 antibody at 7 to 8 months ( $n = 9$  per genotype), 14 months ( $n = 7$  per genotype), or 20 months ( $n = 4$  to 6 per genotype) of age. The hippocampal area occupied by  $A\beta$  deposits was greater in hAPP/hACT than in hAPP mice at all ages examined. Note the lower scale of the  $y$  axis in the youngest age group. Values represent group means  $\pm$  SEM. \*,  $P < 0.05$  versus age-matched hAPP mice (Mann-Whitney  $U$  test).

tive astrocytosis that was most prominent at 20 months of age and of comparable magnitude (data not shown).

#### Similar Transgene Expression and $A\beta$ Production in hAPP/hACT and hAPP Mice before Plaque Formation

The increased plaque load in hAPP/hACT mice could result from effects of hACT on the production, removal, or aggregation of  $A\beta$ . Expression of hAPP and hACT in hAPP/hACT mice did not alter the expression levels of either transgene compared with singly transgenic controls (Figure 2b). To determine whether hACT affects the production or clearance of soluble  $A\beta$ , hippocampal steady-state levels of human  $A\beta_{1-x}$  (approximates total

$A\beta$ ) and  $A\beta_{1-42}$  were measured by enzyme-linked immunosorbent assay.<sup>15</sup> To avoid confounding contributions of  $A\beta$  released from plaques during the homogenization of tissues, these measurements were performed at 5 weeks of age, which is before plaques are detected in hAPP and hAPP/hACT mice. No significant differences were identified between hAPP and hAPP/hACT mice ( $n = 6$  per genotype) in  $A\beta_{1-x}$  ( $42.9 \pm 3.7$  versus  $45.4 \pm 3.0$ ) or  $A\beta_{1-42}$  ( $6.7 \pm 0.4$  versus  $7.1 \pm 0.4$ ) levels (means  $\pm$  SD in nmol/L).  $A\beta_{1-42}/A\beta_{1-x}$  ratios in hAPP and hAPP/hACT mice were also similar ( $0.157 \pm 0.008$  versus  $0.158 \pm 0.008$ ). Thus, hACT does not increase the overall tissue levels of  $A\beta$  before plaque formation.

#### Synaptotoxicity Depends on hAPP/ $A\beta$ but Not on hACT or Plaque Load

One of the best neuropathological correlates of cognitive decline in AD is the loss of SYN-IR presynaptic terminals in specific brain regions.<sup>38-42</sup> Increased expression of  $A\beta$  in PDGF-hAPP mice is associated with a significant decrease in SYN-IR presynaptic terminals in the outer molecular layer of the dentate gyrus.<sup>4,12</sup>

Nontransgenic controls and hACT mice without hAPP/ $A\beta$  expression had comparable levels of SYN-IR presynaptic terminals (Figure 5a), suggesting that expression of hACT does not by itself affect the integrity of these structures. In contrast, hAPP mice with or without hACT expression had decreased levels of SYN-IR presynaptic terminals, but the presence or absence of hACT in these mice did not significantly affect the extent of neurodegeneration (Figure 5a). Similar results were obtained for growth-associated protein 43 (GAP-43) (Figure 5b), another marker of synaptic integrity.<sup>43</sup> No correlation was identified between the density of SYN-IR presynaptic terminals and the hippocampal plaque load in hAPP or hAPP/hACT mice (Figure 5c).

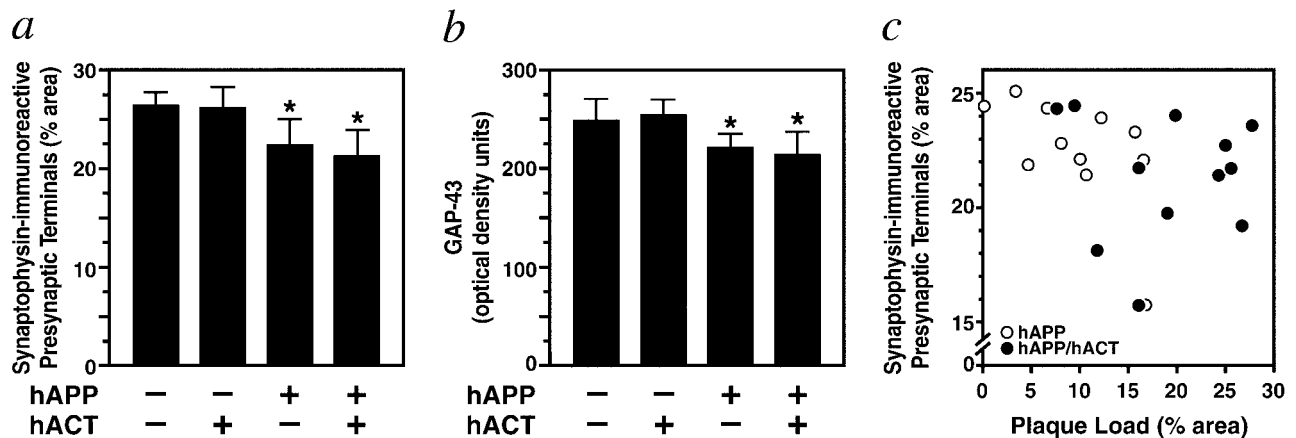


**Figure 5.** Comparable levels of synaptic damage in hAPP and hAPP/hACT mice. The density of SYN-IR presynaptic terminals (a) and the level of GAP-43 immunoreactivity (b) in the molecular layer of the dentate gyrus were determined in nontransgenic controls, singly transgenic mice (hAPP or hACT) and hAPP/hACT doubly transgenic mice ( $n = 11$  to 13 mice per genotype) at 14 to 20 months of age. Data represent group means  $\pm$  SD. \*,  $P < 0.05$  versus nontransgenic controls (Tukey-Kramer test). c: The density of SYN-IR presynaptic terminals did not correlate with the plaque load in hAPP ( $P = 0.074$ ) or hAPP/hACT ( $P = 0.888$ ) mice. At 7 to 8 months of age ( $n = 9$  mice per genotype), the density of SYN-IR presynaptic terminals was also similar in hAPP ( $24.7 \pm 1.4$ ) and hAPP/hACT ( $24.2 \pm 1.9$ ) mice and it did not correlate with plaque load ( $P = 0.76$ ).

## Discussion

We have demonstrated in an hAPP transgenic mouse model that the serpin hACT increases the age-dependent accumulation of cerebral amyloid plaques. This finding may be relevant to AD where hACT is overexpressed in the brain<sup>1</sup> and present in most, if not all, amyloid plaques.<sup>44</sup> Previous studies that examined the effect of hACT on A $\beta$  fibrillization *in vitro* yielded conflicting results.<sup>17,22–26</sup> Our study demonstrates that astroglial overproduction of hACT is clearly amyloidogenic *in vivo*, which suggests that it promotes rather than inhibits the development of AD.

Before plaque formation, similar steady-state levels of A $\beta_{1-x}$  and A $\beta_{1-42}$  were found in the hippocampus of hAPP and hAPP/hACT mice. This indicates that hACT does not increase the production or decrease the degradation of soluble A $\beta$ , at least not in young mice. It is possible that hACT promotes the aggregation of A $\beta$  and its deposition into the brain parenchyma or that it interferes with the degradation and removal of A $\beta$  aggregates. These mechanisms are not mutually exclusive and could involve direct interactions between hACT and A $\beta$ ,<sup>22,23,45</sup> as well as indirect effects of hACT on the levels or activities of extracellular matrix proteins,<sup>46</sup> pathological chaperones,<sup>47</sup> or enzymes that may be involved in the deposition or clearance of amyloid.<sup>48</sup> Additional studies are required to differentiate among these possibilities.

Besides hACT, there are other factors that could influence the deposition of A $\beta$  in AD without affecting A $\beta$  production. Elimination of apolipoprotein E expression by crossing hAPP transgenic mice on the *apoE* knockout background prevents the formation of mature amyloid plaques.<sup>49</sup> Increased astroglial expression of the cytokine transforming growth factor- $\beta$ 1 results in a redistribution of amyloid deposits from the brain parenchyma into blood vessels.<sup>34,50</sup> In contrast, other molecules that have been implicated in the turnover of A $\beta$  by cell culture studies have not had a significant impact on amyloid load when examined in transgenic models. For example, genetic ablation of the class A scavenger receptor did not affect the amyloid burden in the same line of hAPP mice that was analyzed in the current study.<sup>32</sup>

Although there is increasing acceptance of the notion that A $\beta$  plays a pivotal role in AD pathogenesis, the relationship between amyloid plaques and neurodegenerative alterations remains controversial.<sup>51–57</sup> It is interesting in this context that hAPP and hAPP/hACT mice had similar decreases in SYN-IR presynaptic terminals in the dentate gyrus and that the density of these structures did not correlate with the hippocampal plaque load in either group. These findings suggest that A $\beta$ -induced synaptotoxicity is independent of plaque formation, a conclusion supported also by neuropathological studies in humans,<sup>56,57</sup> electrophysiological recordings from hippocampal slices of hAPP mice,<sup>4</sup> and correlations between SYN-IR presynaptic terminals and A $\beta$  levels across multiple lines of hAPP mice.<sup>4,5</sup> In contrast, other AD-associated alterations are likely plaque-dependent. For example, plaques in AD and hAPP mice are tightly associated with dystrophic neurites and reactive

glial cells<sup>5,12,14</sup> and it is possible that neuritic dystrophy<sup>58,59</sup> and glial inflammatory responses<sup>60</sup> contribute to the development of AD dementia. In view of the amyloidogenic effect of hACT observed in the current study, it is tempting to speculate that blocking the production or activity of hACT could inhibit the accumulation of amyloid plaques in the aging brain and, thereby, help prevent the development of plaque-associated alterations.

## Acknowledgments

We thank Dr. F. Checler for A $\beta$  antibodies, Drs. T. Wyss-Coray and K. Weisgraber for helpful comments on the manuscript, G. Howard and S. Ordway for editorial assistance, J. Carroll and S. Gonzales for preparation of graphics, and D. McPherson for administrative assistance.

## References

1. Abraham CR, Selkoe DJ, Potter H: Immunochemical identification of the serine protease inhibitor  $\alpha$ 1-antichymotrypsin in the brain amyloid deposits of Alzheimer's disease. *Cell* 1988, 52:487–501
2. Shoji M, Hirai S, Yamaguchi H, Harigaya Y, Ishiguro K, Matsubara E: Alpha1-antichymotrypsin is present in diffuse senile plaques. A comparative study of beta-protein and alpha1-antichymotrypsin immunostaining in the Alzheimer brain. *Am J Pathol* 1991, 138:247–257
3. Johnson WB, Ruppe MD, Rockenstein EM, Price J, Sarthy VP, Verderber LC, Mucke L: Indicator expression directed by regulatory sequences of the glial fibrillary acidic protein (GFAP) gene: *in vivo* comparison of distinct GFAP-lacZ transgenes. *Glia* 1995, 13:174–184
4. Hsia A, Masliah E, McConlogue L, Yu G, Tatsuno G, Hu K, Kholodenko D, Malenka RC, Nicoll RA, Mucke L: Plaque-independent disruption of neural circuits in Alzheimer's disease mouse models. *Proc Natl Acad Sci USA* 1999, 96:3228–3233
5. Mucke L, Masliah E, Yu G-Q, Mallory M, Rockenstein EM, Tatsuno G, Hu K, Kholodenko D, Johnson-Wood K, McConlogue L: High-level neuronal expression of A $\beta_{1-42}$  in wild-type human amyloid protein precursor transgenic mice: synaptotoxicity without plaque formation. *J Neurosci* 2000, 20:4050–4058
6. Selkoe DJ: Translating cell biology into therapeutic advances in Alzheimer's disease. *Nature* 1999, 399:A23–A31
7. Storey E, Cappai R: The amyloid precursor protein of Alzheimer's disease and the A $\beta$  peptide. *Neuropathol Appl Neurobiol* 1999, 25: 81–97
8. Wilson CA, Doms RW, Lee VM-Y: Intracellular APP processing and A $\beta$  production in Alzheimer disease. *J Neuropathol Exp Neurol* 1999, 58:787–794
9. Gouras GK, Xu HX, Jovanovic JN, Buxbaum JD, Wang R, Greengard P, Relkin NR, Gandy S: Generation and regulation of beta-amyloid peptide variants by neurons. *J Neurochem* 1998, 71:1920–1925
10. Younkin SG: Evidence that A $\beta$ 42 is the real culprit in Alzheimer's disease. *Ann Neurol* 1995, 37:287–288
11. Hosoda R, Saido TC, Otvas LJ, Arai T, Mann DMA, Lee VMY, Trojanowski JQ, Iwatsubo T: Quantification of modified amyloid  $\beta$  peptides in Alzheimer disease and Down-syndrome brains. *J Neuropathol Exp Neurol* 1998, 57:1089–1095
12. Games D, Adams D, Alessandrini R, Barbour R, Berthelette P, Blackwell C, Carr T, Clemens J, Donaldson T, Gillespie F, Guido T, Hagoopian S, Johnson-Wood K, Khan K, Lee M, Leibowitz P, Lieberburg I, Little S, Masliah E, McConlogue L, Montoya-Zavala M, Mucke L, Paganini L, Penniman E, Power M, Schenk D, Seubert P, Snyder B, Soriano F, Tan H, Vitale J, Wadsworth S, Wolozin B, Zhao J: Alzheimer-type neuropathology in transgenic mice overexpressing V717F  $\beta$ -amyloid precursor protein. *Nature* 1995, 373:523–527
13. Rockenstein EM, McConlogue L, Tan H, Gordon M, Power M, Masliah E, Mucke L: Levels and alternative splicing of amyloid  $\beta$  protein



- precursor (APP) transcripts in brains of transgenic mice and humans with Alzheimer's disease. *J Biol Chem* 1995, 270:28257–28267
14. Masliah E, Sisk A, Mallory M, Mucke L, Schenk D, Games D: Comparison of neurodegenerative pathology in transgenic mice overexpressing V717F  $\beta$ -amyloid precursor protein and Alzheimer's disease. *J Neurosci* 1996, 16:5795–5811
  15. Johnson-Wood K, Lee M, Motter R, Hu K, Gordon G, Barbour R, Khan K, Gordon M, Tan H, Games D, Lieberburg I, Schenk D, Seubert P, McConlogue L: Amyloid precursor protein processing and A $\beta_{42}$  deposition in a transgenic mouse model of Alzheimer disease. *Proc Natl Acad Sci USA* 1997, 94:1550–1555
  16. Price DL, Sisodia SS: Mutant genes in familial Alzheimer's disease and transgenic models. *Annu Rev Neurosci* 1998, 21:479–505
  17. Webster S, Rogers J: Relative efficacies of amyloid  $\beta$  peptide (A $\beta$ ) binding proteins in A $\beta$  aggregation. *J Neurosci Res* 1996, 46:58–66
  18. Abraham CR, Shirahama T, Potter H:  $\alpha_1$ -antichymotrypsin is associated solely with amyloid deposits containing the  $\beta$ -protein. Amyloid and cell localization of  $\alpha_1$ -antichymotrypsin. *Neurobiol Aging* 1990, 11:123–129
  19. Potempa J, Korzus E, Travis J: The serpin superfamily of proteinase inhibitors: structure, function, and regulation. *J Biol Chem* 1994, 269:15957–15960
  20. Pasternack JM, Abraham CR, Van Dyke BJ, Potter H, Younkin SG: Astrocytes in Alzheimer's disease gray matter express  $\alpha_1$ -antichymotrypsin mRNA. *Am J Pathol* 1989, 135:827–834
  21. Koo EH, Abraham CR, Potter H, Cork LC, Price DL: Developmental expression of alpha1-antichymotrypsin in brain may be related to astrogliosis. *Neurobiol Aging* 1991, 12:495–501
  22. Ma J, Yee A, Brewer Jr HB, Das S, Potter H: Amyloid-associated proteins  $\alpha_1$ -antichymotrypsin and apolipoprotein E promote assembly of Alzheimer  $\beta$ -protein into filaments. *Nature* 1994, 372:92–94
  23. Janciauskiene S, Eriksson S, Wright HT: A specific structural interaction of Alzheimer's peptide 65  $\beta$ 1-42 with  $\alpha_1$ -antichymotrypsin. *Nat Struct Biol* 1996, 3:668–671
  24. Fraser PE, Nguyen JT, McLachlan DR, Abraham CR, Kirschner DA:  $\alpha_1$ -Antichymotrypsin binding to Alzheimer A $\beta$  peptides is sequence-specific and induces fibril disaggregation *in vitro*. *J Neurochem* 1993, 61:298–305
  25. Eriksson S, Janciauskiene S, Lannfelt L:  $\alpha_1$ -antichymotrypsin regulates Alzheimer  $\beta$ -amyloid peptide fibril formation. *Proc Natl Acad Sci USA* 1995, 92:2313–2317
  26. Hughes SR, Khorkova O, Goyal S, Knaeblein J, Heroux J, Riedel NG, Sahasrabudhe S:  $\alpha_2$ -macroglobulin associates with  $\beta$ -amyloid peptide and prevents fibril formation. *Proc Natl Acad Sci USA* 1998, 95:3275–3280
  27. Ma J, Brewer Jr HB, Potter H: Alzheimer A $\beta$  neurotoxicity: promotion by antichymotrypsin, apoE4; inhibition by A $\beta$ -related peptides. *Neurobiol Aging* 1996, 17:773–780
  28. Aksenov MY, Aksenova MV, Carney JM, Butterfield DA:  $\alpha_1$ -antichymotrypsin interaction with A $\beta$ (1-42) does not inhibit fibril formation but attenuates the peptide toxicity. *Neurosci Lett* 1996, 217:117–120
  29. Aksenova MV, Aksenov MY, Butterfield DA, Carney JM:  $\alpha_1$ -Antichymotrypsin interaction with A $\beta$  (1-40) inhibits fibril formation but does not affect the peptide toxicity. *Neurosci Lett* 1996, 211:45–48
  30. Schubert D: Serpins inhibit the toxicity of amyloid peptides. *Eur J Neurosci* 1997, 9:770–777
  31. Toggas SM, Masliah E, Rockenstein EM, Rall GF, Abraham CR, Mucke L: Central nervous system damage produced by expression of the HIV-1 coat protein gp120 in transgenic mice. *Nature* 1994, 367:188–193
  32. Huang F, Buttini M, Wyss-Coray T, McConlogue L, Kodama T, Pitas RE, Mucke L: Elimination of the class A scavenger receptor does not affect amyloid plaque formation or neurodegeneration in transgenic mice expressing human amyloid protein precursors. *Am J Pathol* 1999, 155:1741–1749
  33. Wyss-Coray T, Feng L, Masliah E, Ruppe MD, Lee HS, Toggas SM, Rockenstein EM, Mucke L: Increased central nervous system production of extracellular matrix components and development of hydrocephalus in transgenic mice overexpressing transforming growth factor- $\beta$ 1. *Am J Pathol* 1995, 147:53–67
  34. Wyss-Coray T, Masliah E, Mallory M, McConlogue L, Johnson-Wood K, Lin C, Mucke L: Amyloidogenic role of cytokine TGF- $\beta$ 1 in transgenic mice and Alzheimer's disease. *Nature* 1997, 389:603–606
  35. Barelli H, Lebeau A, Vizzavona J, Deleare P, Chevallier N, Drouot C, Marambaud P, Ancolio K, Buxbaum JD, Khorkova O, Heroux J, Sahasrabudhe S, Martinez J, Warter J-M, Mohr M, Checler F: Characterization of new polyclonal antibodies specific for 40 and 42 amino acid-long amyloid  $\beta$  peptides: their use to examine the cell biology of presenilins and the immunohistochemistry of sporadic Alzheimer's disease and cerebral amyloid angiopathy cases. *Mol Med* 1997, 3:695–707
  36. Mucke L, Masliah E, Johnson WB, Ruppe MD, Alford M, Rockenstein EM, Forss-Petter S, Pietropaolo M, Mallory M, Abraham CR: Synaptotrophic effects of human amyloid  $\beta$  protein precursor in the cortex of transgenic mice. *Brain Res* 1994, 666:151–167
  37. Buttini M, Orth M, Bellosta S, Akeefe H, Pitas RE, Wyss-Coray T, Mucke L, Mahley RW: Expression of human apolipoprotein E3 or E4 in the brains of *Apoe*<sup>-/-</sup> mice: isoform-specific effects on neurodegeneration. *J Neurosci* 1999, 19:4867–4880
  38. Terry RD, Masliah E, Salmon DP, Butters N, DeTeresa R, Hill R, Hansen LA, Katzman R: Physical basis of cognitive alterations in Alzheimer's disease: synapse loss is the major correlate of cognitive impairment. *Ann Neurol* 1991, 30:572–580
  39. Honer WG, Dickson DW, Glesson J, Davies P: Regional synaptic pathology in Alzheimer's disease. *Neurobiol Aging* 1992, 13:375–382
  40. Masliah E, Mallory M, Hansen L, DeTeresa R, Alford M, Terry R: Synaptic and neuritic alterations during the progression of Alzheimer's disease. *Neurosci Lett* 1994, 174:67–72
  41. Dickson DW, Crystal HA, Bevana C, Honer W, Vincent I, Davies P: Correlations of synaptic and pathological markers with cognition of the elderly. *Neurobiol Aging* 1995, 16:285–298
  42. Sze CI, Troncoso JC, Kawas C, Mouton P, Price DL, Martin LJ: Loss of the presynaptic vesicle protein synaptophysin in hippocampus correlates with cognitive decline in Alzheimer disease. *J Neuropathol Exp Neurol* 1997, 56:933–944
  43. Masliah E, Fagan A, Terry R, DeTeresa R, Mallory M, Gage R: Reactive synaptogenesis assessed by synaptophysin immunoreactivity is associated with GAP43 in the dentate gyrus of the adult rat. *Exp Neurol* 1991, 113:131–142
  44. Rozemuller JM, Abbink JJ, Kamp AM, Stam FC, Hack CE, Eikelenboom P: Distribution pattern and functional state of  $\alpha_1$ -antichymotrypsin in plaques and vascular amyloid in Alzheimer's disease. *Acta Neuropathol* 1991, 82:200–207
  45. Janciauskiene S, Rubin H, Lukacs CM, Wright HT: Alzheimer's peptide A $\beta_{1-42}$  binds to two  $\beta$ -sheets of  $\alpha_1$ -antichymotrypsin and transforms it from inhibitor to substrate. *J Biol Chem* 1998, 273:28360–28364
  46. Snow AD, Sekiguchi R, Nochlin D, Fraser P, Kimata K, Mizutani A, Arai M, Schreier WA, Morgan DG: An important role of heparan sulfate proteoglycan (perlecan) in a model system for the deposition and persistence of fibrillar  $\alpha$ -amyloid in rat brain. *Neuron* 1994, 12:219–234
  47. Wisniewski T, Frangione B: Apolipoprotein E: a pathological chaperone protein in patients with cerebral and systemic amyloid. *Neurosci Lett* 1992, 135:235–238
  48. Yamin R, Malgeri EG, Sloane JA, McGraw WT, Abraham CR: Metalloendopeptidase EC 3.4.24.15 is necessary for Alzheimer's amyloid- $\beta$  peptide degradation. *J Biol Chem* 1999, 274:18777–18784
  49. Bales KR, Verina R, Dodel RC, Du R, Altstiel L, Bender B, Hyslop P, Johnstone EM, Little SP, Cummins DJ, Piccardo P, Ghetti B, Paul SM: Lack of apolipoprotein E dramatically reduces amyloid  $\beta$ -peptide deposition. *Nat Genet* 1997, 17:263–264
  50. Wyss-Coray T, Lacombe P, Von Euw D, Lin C, McConlogue L, Masliah E, Mucke L: TGF- $\beta$ 1 modulates brain amyloid deposition and induces Alzheimer's disease like microvascular abnormalities in transgenic mice. *Soc Neurosci Abstr* 1999, 25:22
  51. Cummings BJ, Pike CJ, Shankle R, Cotman CW:  $\beta$ -amyloid deposition and other measures of neuropathology predict cognitive status in Alzheimer's disease. *Neurobiol Aging* 1996, 17:921–933
  52. Terry RD: The pathogenesis of Alzheimer disease: an alternative to the amyloid hypothesis. *J Neuropathol Exp Neurol* 1996, 55:1023–1025
  53. Bartoo GT, Nochlin D, Chang D, Kim Y, Sumi SM: The mean A $\beta$  load in the hippocampus correlates with duration and severity of dementia in subgroups of Alzheimer disease. *J Neuropathol Exp Neurol* 1997, 56:531–540

54. Davis JN, Chisholm JC: The 'amyloid cascade hypothesis' of AD: decoy or real McCoy? *Trends Neurosci* 1997, 20:558–559
55. Gomez-Isla T, Hollister R, West H, Mui S, Growdon JH, Petersen RC, Parisi JE, Hyman BT: Neuronal loss correlates with but exceeds neurofibrillary tangles in Alzheimer's disease. *Ann Neurol* 1997, 41:17–24
56. Lue L-F, Kuo Y-M, Roher AE, Brachova L, Shen Y, Sue L, Beach T, Kurth JH, Rydel RE, Rogers J: Soluble amyloid  $\beta$  peptide concentration as a predictor of synaptic change in Alzheimer's disease. *Am J Pathol* 1999, 155:853–862
57. McLean CA, Cherny RA, Fraser FW, Fuller SJ, Smith MJ, Beyreuther K, Bush AI, Masters CL: Soluble pool of A $\beta$  amyloid as a determinant of severity of neurodegeneration in Alzheimer's disease. *Ann Neurol* 1999, 46:860–866
58. Knowles RB, Gomez-Isla T, Hyman BT: A $\beta$  associated neuropil changes: correlation with neuronal loss and dementia. *J Neuropathol Exp Neurol* 1998, 57:1122–1130
59. Knowles RB, Wyart C, Buldyrev SV, Cruz L, Urbanc B, Hasselmo ME, Stanley HE, Hyman BT: Plaque-induced neurite abnormalities: implications for disruption of neural networks in Alzheimer's disease. *Proc Natl Acad Sci USA* 1999, 96:5274–5279
60. Akiyama H, Barher S, Barnum S, Bradt B, Bauer J, Cooper NR, Eikelenboom P, Emmerling M, Fiebich B, Finch CE, Frautschy S, Griffin WST, Hampel H, Landreth G, McGeer PL, Mrak R, McKenzie I, O'Banion K, Pachter J, Pasinetti G, Plata-Salaman C, Rogers J, Rydel R, Shen Y, Streit W, Strohmeyer R, Tooyama I, Van Muiswinkel FL, Veerhuis R, Walker D, Webster S, Wegrzyniak B, Wenk G, Wyss-Coray T: Inflammation and Alzheimer's disease. Neuroinflammation working group. *Neurobiol Aging* 2000, 21:383–421